Colloids and Surfaces B: Biointerfaces 84 (2011) 427–432

Contents lists available at ScienceDirect

Colloids and Surfaces B: Biointerfaces

journal homepage: www.elsevier.com/locate/colsurfb

A novel amperometric hydrogen peroxide biosensor based on immobilized Hb in Pluronic P123-nanographene platelets composite

X.X. Xu[a], J.X. Zhang[a], F. Guo[a], W. Zheng[a,**], H.M. Zhou[a], B.L. Wang[a], Y.F. Zheng[a,b,*], Y.B. Wang[b,c], Y. Cheng[c], X. Lou[a,d], B.Z. Jang[e]

[a] Center for Biomedical Materials and Engineering, Harbin Engineering University, Harbin 150001, China
[b] Department of Advanced Materials and Nanotechnology, College of Engineering, Peking University, Beijing 100871, China
[c] Center for Biomedical Materials and Tissue Engineering, Academy for Advanced Interdisciplinary Studies, Peking University, Beijing 100871, China
[d] Department of Chemical Engineering, Curtin University of Technology, Kent Street, Bentley, WA 9102, Australia
[e] College of Engineering and Computer Science, Wright State University, 3640 Colonel Glenn Hwy., Dayton, OH 45435, USA

ARTICLE INFO

Article history:
Received 4 December 2010
Received in revised form 23 January 2011
Accepted 23 January 2011
Available online 2 February 2011

Keywords:
Biosensor
Hemoglobin
Nanographene platelets
Direct electron transfer
Electrocatalysis

ABSTRACT

In this paper, an amperometric biosensor of hydrogen peroxide (H_2O_2) was fabricated by immobilization of Hemoglobin (Hb) on a Pluronic P123-nanographene platelet (NGP) composite. Direct electron transfer in the Hb-immobilized P123-NGP composite film was greatly facilitated. The surface concentration (Γ^*) and apparent heterogeneous electron transfer rate constant (k_s) were calculated to be $(1.60 \pm 0.17) \times 10^{-10}$ mol cm^{-2} and 48.51 s^{-1}, respectively. In addition, the Hb/Pluronic P123-NGP composite showed excellent bioelectrocatalytic activity toward the reduction of H_2O_2. The biosensor of H_2O_2 exhibited a linear response to H_2O_2 in the range of 10–150 μM and a detection limit of 8.24 μM (S/N = 3) was obtained. The apparent Michaelis–Menten constant (K_m^{app}) was 45.35 μM. The resulting biosensor showed fast amperometric response, with very high sensitivity, reliability and effectiveness.

1. Introduction

Electrochemical biosensors are self-contained integrated devices, which are capable of providing specific quantitative or semi-quantitative analytical information using a biological recognition element (biochemical receptor) and an electrochemical transduction element. Over the past years, considerable attention has been paid to the research of electrochemical biosensor, due to their high sensitivity and selectivity, fast response, low cost, and the potential for continuous on-line detection of complex systems [1]. Enzyme electrodes are one of the earliest developed and most commonly used electrochemical biosensors, which are based on direct electron transfer between the electrode and the redox activity center of an enzyme [2–4]. One of the major issues when working with enzymes is their stability. This includes both self and operational stability. Another problem associated with enzyme electrodes is their rather slow heterogeneous electron transfer rates. The following three facts and/or the combination of them can be the major causes of the low electron transfer rate: (1) the electroactive prosthetic groups are often deeply buried within the complex structure of enzymes; (2) the enzymes adsorbed on the electrodes might have been denatured; and (3) the orientations of the enzymes on the electrodes might be unfavorable to the electron transfer [5,6]. Enzyme immobilization has become a vital step in overcoming these problems [7–11].

Nanomaterials and nanotechnologies have been widely studied and used in the sensor development because of their novel optical, electrical and catalytic properties, and favorable biocompatibility. Improved performance of the resulting biosensors has been reported when nanoplated bismuth titanate sub-microspheres [7], Fe_3O_4 nanoparticles [8], titanium oxide nanotubes [9] and a few other nanomaterials [12–17], are utilised in the fabrication of biosensor.

Nanoscale graphene platelets or graphene nanosheets are composed of two-dimensional nanosized graphene fragments with honeycomb lattice [18]. Due to the presence of the closed π-electron systems and the two-dimensional extended electronic structure of π-electrons with open edges, these materials possess unique electronic transport and mechanical properties, and great

* Corresponding author at: Department of Advanced Materials and Nanotechnology, College of Engineering, Peking University, Beijing 100871, China. Tel.: +86 10 6276 7411; fax: +86 10 6276 7411.
** Co-corresponding author at: Center for Biomedical Materials and Engineering, Harbin Engineering University, No. 145, Na-Tong-Da Street, Nan-Gang District, Harbin 150001, China. Tel.: +86 451 8251 8644; fax: +86 451 8251 8644.
E-mail addresses: zhengwei75@126.com (W. Zheng), yfzheng@pku.edu.cn (Y.F. Zheng).

0927-7765/$ – see front matter © 2011 Elsevier B.V. All rights reserved.
doi:10.1016/j.colsurfb.2011.01.037

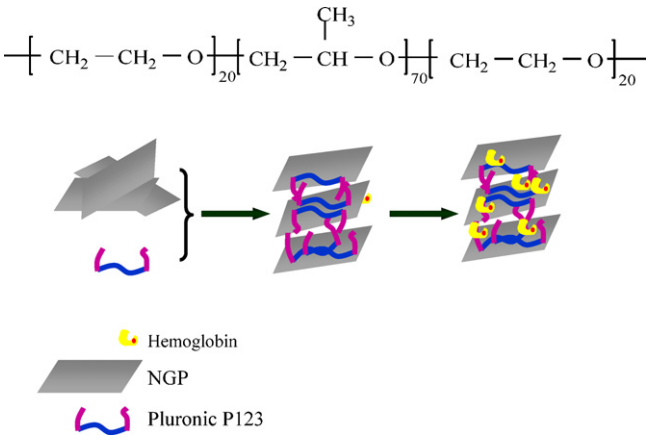

Scheme 1. Chemical structure of the Pluronic P123 and schematic of the immobilization of Hb in Pluronic P123-NGP composite.

thermal and electrical conductivities. They have been studied as a supporting platform for fabricating electrochemical biosensors and biomedical devices, as reported in many review articles [19–23]. On the other hand, Pluronic P123 is an important amphiphilic block copolymer and has been widely used as a biomaterial for its superior biocompatibility [24–26]. It can be used as a suitable matrix for enzyme immobilization [27].

The detection of hydrogen peroxide (H_2O_2) is of great importance because it is an essential chemical used or produced in various industrial processes and applications including biomedical, biological, pharmaceutical and environmental systems. It has a significant impact on our daily life and health. Traditional methods developed for determining hydrogen peroxide include titrimetry, spectrometry, chemiluminescence and electrochemical approaches. Amperometric enzyme-based biosensors for the determination of H_2O_2 coupled with the intrinsic selectivity and sensitivity of enzymatic reactions have received considerable interest because of their good sensitivity, high selectivity and convenience [28,29]. In this paper, we propose to fabricate an amperometric enzyme-based biosensor to determinate H_2O_2. We will use nanographene platelets to improve the stability and sensitivity of the developed biosensor.

2. Experiments

2.1. Materials

Nanographene platelet (NGP) was provided by Prof. B.Z. Jang (Wright State University, USA). They were dried under vacuum at 100 °C for 24 h to remove the residual organic solvent prior to use. The PEO–PPO–PEO block copolymers, Pluronic P123 (M_w 5800), were purchased from Aldrich-China and used as received. Pluronic P123 is presented as $EO_{20}PO_{70}EO_{20}$ (Scheme 1) on the basis of its molecular weight and PEO content (36 wt.%). Hemoglobin (Hb) (from bovine blood, M_w 66,000, the isoelectric point p$I \sim 7.4$ [30]) was purchased from Sigma Chemical Co. as lyophilized powder, and was used without further purification. A solution of Hb (20 mg mL^{-1}) was prepared using 0.10 mol L^{-1} phosphate buffer solutions (pH 7.0). The hydrogen peroxide (H_2O_2, 30%, w/w) was purchased from Beijing Chemical Company (Beijing, China). Fresh dilutions of H_2O_2 were prepared daily for the experiments. Potassium dihydrogen orthophosphate (0.10 mol L^{-1}) was used to prepare the supporting electrolyte and its pH value was adjusted using KOH solution. All other chemicals and solvents were of analytical grade and used without further purification. All aqueous solutions were prepared using double-distilled water.

2.2. Preparation of biosensor

Prior to coating, the bare glassy carbon (GC, 3 mm-diameter) electrode was first polished with emery paper (# 2000), 0.3 μm and 0.05 μm alumina slurry on a woolen cloth, then cleaned in a ultrasonic bath for 10 min and finally thoroughly rinsed with double-distilled water. The NGP was dispersed into 2.0 mg mL^{-1} aqueous solution of Pluronic P123 and the mixture was ultrasonicated for 1 h to obtain a homogeneous and black dispersion.

For the preparation of Hb/P123-NGP/GC electrodes, 4 μL of the P123-NGP dispersion was dip-coated onto the pretreated GC electrodes, and dried in air. Subsequently, the P123-NGP/GC electrodes were immersed in a 20 mg mL^{-1} Hb solution for 4 h and coated with 2 μL of the Nafion solution (5 wt.%) to form a tight membrane on the enzyme electrodes. The resulting electrodes (denoted as Hb/P123-NGP/GC) were rinsed with double-distilled water prior to electrochemical measurements. These enzyme electrodes were stored at 4 °C in a refrigerator when not in use.

2.3. Electrochemical measurements

All the electrochemical measurements were carried out using a computer-controlled electrochemical analyzer (CHI 650C, Chen-Hua, Shanghai). A conventional three-electrode cell was used in the electrochemical measurements. The prepared Hb/P123-NGP/GC electrode was used as the working electrode, a platinum spiral wire as the counter electrode and a saturated calomel electrode (SCE) as the reference electrode. The electrochemical impedance spectra were recorded at a basis potential of 0.20 V within the frequency range of 10^{-2} to 10^6 Hz in 5.0 mM $K_3Fe(CN)_6$ containing 0.10 M KCl. The amplitude of the applied sine wave at the basis potential in each case was 5 mV. To maintain the anaerobic conditions under which the experiments were conducted, the electrolyte was bubbled with pure nitrogen gas for more than 30 min prior to electrochemical measurements, and nitrogen gas was kept flowing over the solution during all electrochemical measurements. All electrochemical measurements were performed at least three times at room temperature (25 ± 2 °C). In order to ensure the reproducibility of the experimental results, five enzyme electrodes were prepared for each electrochemical measurement.

3. Results and discussion

3.1. Characterization of NGP and Hb/P123-NGP film

The morphology of NGP was characterized by TEM. Fig. 1A shows the typical TEM images of NGP, which clearly illustrates the flake-like shapes of graphene with corrugation and scrolling because of microscopic crumpling via bending or buckling of the two-dimensional membrane [31,32]. The edges of NGP were extremely thin (<1 nm). Fig. 1B shows the electrochemical impedance spectra of the P123-NGP modified GC electrodes with different Pluronic P123 concentrations in 5.0 mM $K_3Fe(CN)_6$ containing 0.10 M KCl. It can be seen that the heterogeneous electron transfer resistance of the P123-NGP/GC electrodes with the same amount of P123-NGP containing 2.0 mg mL^{-1} NGP increased greatly with the increase of the Pluronic P123 concentrations. Pluronic P123 is a typical amphiphilic block copolymer which could induce higher interactions between different interfaces. However, the heterogeneous electron transfer procedure on the P123-NGP modified GC electrodes may be blocked due to the insulating properties of the block copolymer. Tapping mode AFM was used to investigate the surface of the immobilization of Hb on P123-NGP. As shown in Fig. 1C, the aggregated Hb molecules on P123-NGP and some nanosized islands were observed.

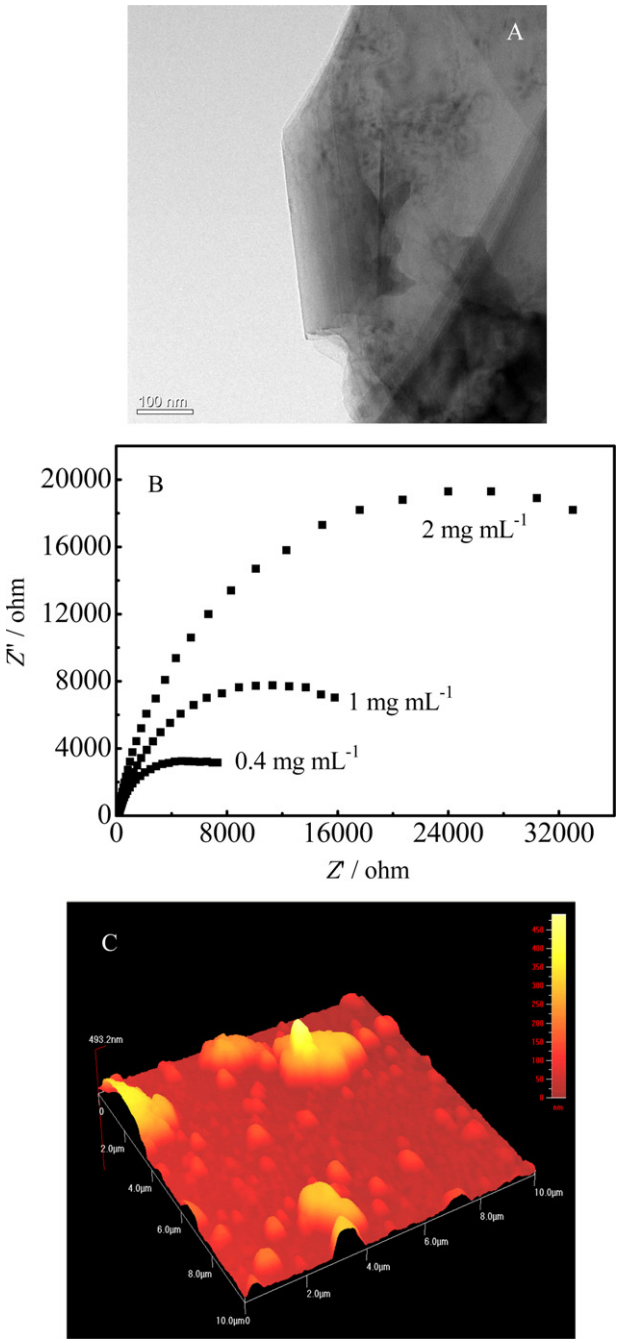

Fig. 1. (A) TEM image of NGP. (B) Electrochemical impedance spectra obtained at the P123-NGP modified GC electrodes with different P123 concentrations in 5.0 mM $K_3Fe(CN)_6$ containing 0.10 M KCl. (C) AFM image of the Hb adsorbed on P123-NGP.

3.2. Direct electrochemistry of Hb immobilized P123-NGP film

Fig. 2 shows the typical cyclic voltammograms (CVs) of the Hb/P123-NGP/GC (solid line) and P123-NGP/GC (dashed line) modified electrodes in a 0.10 M N_2-saturated phosphate buffer solution of pH 7.0 at a scan rate of 100 mV s^{-1}, respectively. As can be seen from this figure, a pair of well-defined redox peaks were observed at the Hb/P123-NGP/GC electrode with the potentials as $E_{pc} = -0.40$ V and $E_{pa} = -0.27$ V (vs. SCE), but no redox peak was observed for the P123-NGP/GC electrode. Moreover, the formal potential was −0.335 V (vs. SCE) which was consistent with the reported values for the Fe(III)/Fe(II) redox center of the heme group of the Hb [33,34]. These results indicated that the direct electron transfer

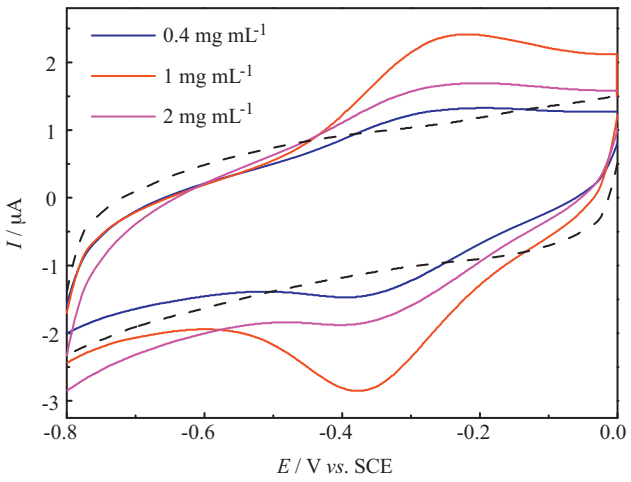

Fig. 2. Cyclic voltammograms (CVs) obtained at a P123-NGP/GC electrode (dashed line) and a Hb/P123-NGP/GC electrode (solid line) with different P123 concentrations in a 0.10 M N_2-saturated phosphate buffer solution.

between Hb and underlying electrode could be easily facilitated by the P123-NGP assembling onto GC electrode. The reason can be explained as follows. On one hand, the Pluronic P123 endowed the Hb to maintain its suitable conformation and activity [27] and the NGP possessed good electrical conductivity with high surface area. On the other hand, the hydrophobic PPO segments of Pluronic P123 could be adsorbed onto the NGP through hydrophobic interaction. In addition, the two hydrophilic PEO segments would cause the separation of the nanographene platelets and produce more space between nanographene layers, as shown in Scheme 1. Therefore, a larger number of Hb were immobilized within nanographene layers, which made the surface concentration of the electroactive Hb increase. Hence, it can be concluded that the assembling of Pluronic P123-dispersed NGTs onto an electrode is useful for facilitating the electron transfer of the proteins.

It is also found that the electrochemical behavior of Hb is affected by the concentration of Pluronic P123. For the Hb/P123-NGP/GC electrodes with the same amount of the P123-NGP dispersion containing 2.0 mg mL^{-1} NGP and different concentrations of P123, the anodic and cathodic peak currents were remarkably larger when the concentration of P123 in 2.0 mg mL^{-1} NGP dispersed solution was 1.0 mg mL^{-1}. Hence, the optimal amount of 1.0 mg mL^{-1} P123 in 2.0 mg mL^{-1} NGP dispersed solution was selected for the following experiments.

Fig. 3 shows the effect of scan rate on the electrochemical responses of Hb immobilized on the P123-NGP film. As can be seen from Fig. 3A, the cathodic and anodic peak potentials exhibited a small shift caused by the increase of the scan rate (v). At the same time, the peak current (I_p) increased along with the rising of scan rate from 100 mV s^{-1} to 900 mV s^{-1} (inset of Fig. 3A). This demonstrated that the electron transfer between Hb and the electrode was a typical quasi-reversible and surface-controlled electrochemical process [30]. The surface concentration (Γ^*) of the electroactive Hb in the P123-NGP film was estimated to be $(1.60 \pm 0.17) \times 10^{-10}$ mol cm^{-2} by Faraday's law, $Q = nFA\Gamma^*$ (F is Faraday's constant, Q can be obtained by integrating the cathodic peak of Hb, n and A stand for the number of electron transferred and the area of the electrode surface, respectively) with the integration of the Fe^{III} reduction peaks at the scan rate of 100–500 mV s^{-1}. This value was much larger than that of the theoretical monolayer coverage of Hb on the surface of the GC electrode (1.89×10^{-11} mol cm^{-2}), suggesting that multi-layers of Hb were entrapped in the P123-NGP film, which could participate in the electron transfer process. In addition, we further investigated

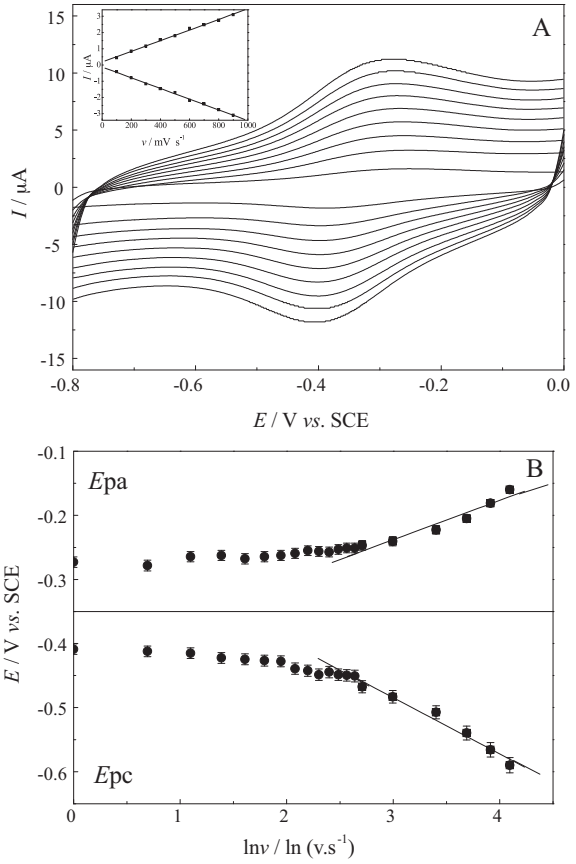

Fig. 3. (A) CVs obtained at the Hb/P123-NGP/GC electrode in 0.10 M N_2-saturated phosphate buffer solution at 100, 200, 300, 400, 500, 600, 700, 800 and 900 mV s^{-1} (from inner to outer), respectively. Inset shows a plot of cathodic and anodic peak currents against the scan rate of potential. (B) Plots of anodic peak potentials and cathodic peak potentials against the logarithm of scan rate. Data are shown as mean ± SD (n = 5).

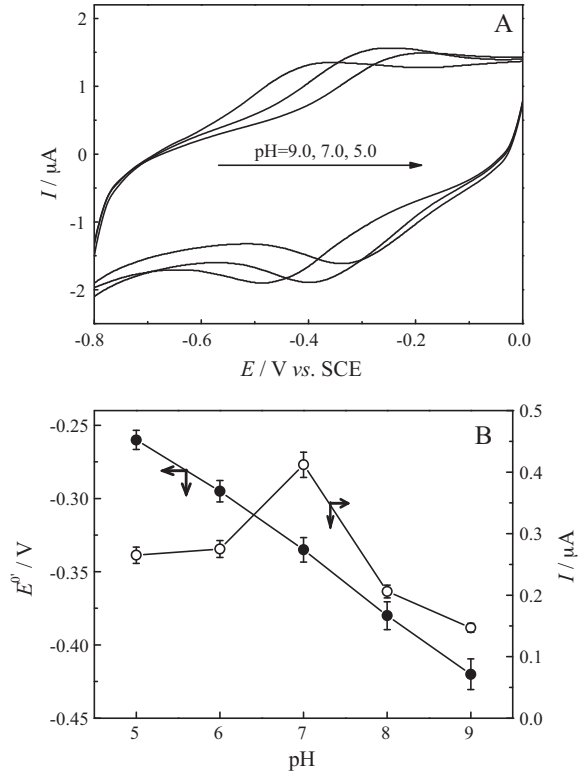

Fig. 4. (A) CVs for Hb/P123-NGP/GC electrodes at different pH values of phosphate buffer solutions. (B) Dependence of peak currents (○) and formal potentials ($E^{0\prime}$) (●) on the pH values of phosphate buffer solutions. Scan rate, 100 mV s^{-1}. Data are shown as mean ± SD (n = 5).

the electrochemical kinetic parameter k_s (the apparent heterogeneous electron transfer rate constant) in detail, which can be easily calculated using the Laviron's equations [35] according to the relationship between ΔE_p and v (Fig. 3B). The k_s of Hb confined in the P123-NGP film was evaluated to be 48.51 s^{-1} and was markedly higher than 1.72 s^{-1} for Hb/P123 modified electrode [27], 9.54 ± 0.88 s^{-1} for Hb/SA-MWCNTs electrode [36], and 5.05 ± 0.41 s^{-1} for Hb/MWCNTs-HA modified electrode [37]. This is because the NGP could act as the electron bridge or connector between the Hb molecules and the underlying electrode with a relatively large distance. Meanwhile, the P123 copolymer film can provide a favorable microenvironment for Hb to retain its biological activity [27]. Therefore, it can be demonstrated again that the use of the P123-NGP film enhanced the electron transfer rate between the immobilized Hb and the GC electrode.

The effect of the pH value on the electrochemical behavior of Hb in the P123-NGP film had also been investigated. Fig. 4 shows CVs of Hb/P123-NGP/GC electrode at different pH values and the dependence of peak current and formal potential ($E^{0\prime}$) on the pH value of buffer solution. As can be seen, the negative shift of potentials of both reduction and oxidation peaks was observed with the increase of the pH value (from 5.0 to 9.0) in the solution. Moreover, the formal potential ($E^{0\prime}$) exhibited a linear relationship with the pH value, the slope of which was −40.5 mV pH^{-1} (Fig. 4B). This value was smaller than the theoretical value of −59.2 mV pH^{-1} for the reaction of one electron coupled with one proton, and is in agreement with the results reported by others [38,39]. Furthermore, it also can be seen from Fig. 4B, the peak current increased with the pH value of the supporting electrolyte from 5.0 to 7.0, and then decreased steeply when the pH value further increased to 9.0. The reason could be attributed to the protonation states of the trans ligands of the heme iron and amino acids around the heme, or the protonation of the water molecule coordinated to the central iron [40,41], which can increase the barrier for the electron transfer [42,43]. Thus, the phosphate buffer solution with the pH value of 7.0 was selected as the supporting electrolyte in the following experiments.

3.3. H_2O_2 biosensor based on Hb immobilized P123-NGP

The intrinsic selectivity and sensitivity of the enzymatic reaction is promising for the fabrication of simple and low-cost enzyme biosensors. Hb could be used to reduce the oxygen and hydrogen peroxide through electrochemical catalysis because it has structural similarity to the peroxidase with an intrinsic catalytic activity toward peroxide compounds [44,45]. In order to explore the electrocatalytic activity of Hb in the P123-NGP modified electrode, we investigated the bioelectrocatalytic reduction behavior toward H_2O_2 using the cyclic voltammograms and amperometric technique upon the successive additions of H_2O_2 in phosphate buffer solution. Fig. 5 shows the CVs of Hb/P123-NGP/GC electrode in 0.10 M pH 7.0 phosphate buffer solution containing different contents of H_2O_2. As can be seen, when the H_2O_2 was added into phosphate buffer solution, the cathodic peak currents at about −0.40 V (vs. SCE) increased dramatically with the decrease of the anodic peak (dashed line) for the Hb/P123-NGP/GC modified electrode. Moreover, the cathodic current peaks gradually increased with the increase of the concentration of H_2O_2. These results indicated that the immobilized Hb exhibited excellent electrocatalytic activity toward the reduction of H_2O_2.

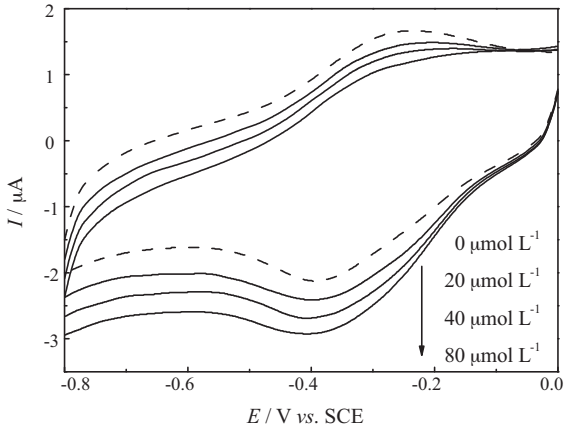

Fig. 5. CVs for Hb/P123-NGP/GC electrodes in a 0.10 M pH 7.0 phosphate buffer solution containing different contents of H_2O_2. Scan rate, 100 mV s^{-1}.

The mechanisms can be explained as follows [46]:

$$\text{Hb}\quad (Fe^{3+}) + H_2O_2 \rightarrow \text{Compound}\quad \text{I}\quad (Fe^{4+}{=}O) + H_2O$$

$$\text{Compound}\quad \text{I}\quad (Fe^{4+}{=}O) + e + H^+ \rightarrow \text{Compound}\quad \text{II}$$

$$\text{Compound}\quad \text{II} + e + H^+ \rightarrow \text{Hb}\quad (Fe^{3+}) + H_2O$$

In addition, we systematically investigated the performance of the biosensor based on the immobilized Hb on P123-NGP film. Fig. 6A shows the amperometric responses of the Hb/P123-NGP/GC modified electrodes upon the successive additions of H_2O_2 in the phosphate buffer solution (0.10 M, pH 7.0) at an applied potential of −0.40 V (vs. SCE). It can be seen that the steady-state response current of the biosensor increased obviously with the increase of the H_2O_2 concentration. Moreover, the linear range of the response was in the range of 10–150 μM (Fig. 6B) which can be described by a linear regression equation of $\Delta I/\text{nA} = -110.7 + 15.27C/\mu\text{M}$ with the correlation coefficient of 0.997 ($n = 7$). In addition, the detection limit of the biosensor was calculated to be 8.24 μM at a signal-to-noise ratio of 3. The performance of the present H_2O_2 biosensor was compared with the previous work of H_2O_2 biosensor, as shown in Table 1. As can be seen, the performance of the present H_2O_2 biosensor based on the Hb/P123-NGP/GC modified electrode was comparable with those reported previously. When H_2O_2 concentration was higher than 150 μM, a response plateau was observed, representing the feature of the Michaelis–Menten kinetic mechanism (inset in Fig. 6). The apparent Michaelis–Menten constant (K_m^{app}) can be calculated according to the Lineweaver–Burk form of the Michaelis–Menten equation [51]: $1/I_{ss} = (1/I_{max}) + (K_m^{app}/I_{max}c)$. Here I_{ss} is the steady-state current after the addition of a substrate and can be obtained from amperometric experiment; I_{max} is the maximum current under saturated substrate condition; c is the concentration of the substrate. The K_m^{app} value was calculated to be 45.35 μM, which was markedly smaller than that reported previously in the literature [8,47,49,52–56]. Moreover, it is more important that this K_m^{app} value was less than that of the biosensor based on the direct electrochemistry of Hb incorporated in PEO–PPO–PEO triblock copolymer film by one order of magnitude [27]. It is well known that a lower value of K_m^{app} implies higher catalytic activity of the immobilized enzyme to the substrate, thus it can be concluded that the immobilization of Hb in P123-NGP interface retains its bioactivity and possesses a high biological affinity to H_2O_2.

Table 1
Linear range and detection limit for different H_2O_2 biosensors based on the direct electron transfer of Hb.

Different H_2O_2 biosensors	Linear range (μM)	Detection limit (μM)	Reference
Hb/P123-NGP	10–150	8.24	This work
Hb/AuNPs-C@SiO_2	5–80	0.08	[47]
Hb/ZnO-MWCNTs/Nafion	0.2–12	0.084	[48]
Hb/CuO-NWBs	10–90	3.3	[49]
Hb/Fe_3O_4-CS	5–90	0.5	[50]
Hb/CMC-TiO_2-NT	4–64	4.637	[9]
Hb/NGC-SF	600–1700	100	[16]

CS, chitosan; CMC, carboxymethyl cellulose; NGC-SF, nanostructured gold colloid-silk fibroin.

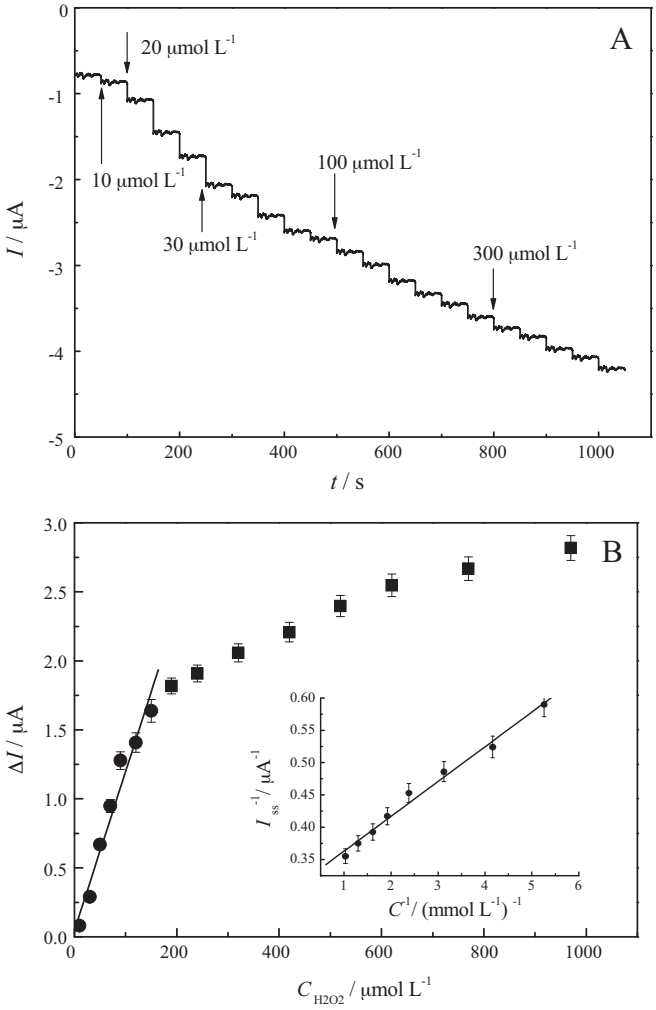

Fig. 6. (A) Amperometric responses of Hb/P123-NGP/GC electrode in stirred solutions to the successive additions of H_2O_2. Applied potential: −0.40 V vs. SCE; supporting electrolyte: 0.10 M pH 7.0 phosphate buffer solution. (B) The calibration plot of catalytic peak current vs. the concentrations of H_2O_2. Inset is the corresponding Lineweaver–Burk plot. Data are shown as mean ± SD ($n = 5$).

3.4. Stability and real samples assay

Finally, to further assess the possible application of our proposed method, the stability and the real analytical usefulness were investigated. Over 85% response of its initial sensitivity to the reduction of H_2O_2 can be retained after the biosensor had been stored in a 0.10 M phosphate buffer for 2 weeks at 4 °C, showing its good long-term stability. The reproducibility of the biosensor was examined using a H_2O_2 solution of 20 μM, and the relative standard deviation was approximately 3.52% for five successive assays. In addition, a series of H_2O_2 solutions containing different disinfectant sam-

Table 2
Determination of H_2O_2 in different samples ($n = 5$).

Groups	Detected (mol L^{-1})	Found (mol L^{-1})
1	0.72 ± 0.077	0.667
2	0.76 ± 0.065	0.769
3	1.05 ± 0.077	1.00

ples were prepared by mixing hydrogen peroxide solutions with different contents using the standard addition method. The concentrations of H_2O_2 in disinfectant samples were measured using the method proposed above as shown in Table 2. It can be seen that the values obtained using the proposed method were consistent with those founded. The relative standard deviation was about 7% indicating that the present method is quite reliable and effective in practical detection.

4. Conclusions

In the present paper, an amperometric biosensor of H_2O_2 was fabricated by immobilizing Hb onto the Pluronic P123-NGP composite to improve the long-term stability and the sensitivity of biosensors. Direct electron transfer in the Hb immobilized P123-NGP composite film was greatly facilitated and showed the excellent bioelectrocatalytic activity toward the reduction of hydrogen peroxide. Moreover, the established biosensor showed fast amperometric response, with very high sensitivity, reliability and effectiveness.

Acknowledgements

This work was supported by the National Natural Science Foundation of China (No. 20805010) and the Fundamental Research Funds for the Central Universities (No. HEUCF101021).

References

[1] A.P.F. Turner, Science 290 (2000) 1315–1317.
[2] S.J. Updike, G.P. Hicks, Nature 214 (1967) 986–988.
[3] L.C. Clark, C. Lyons, Ann. N.Y. Acad. Sci. 102 (1962) 29–45.
[4] E.-H. Yoo, S.-Y. Lee, Sensors 10 (2010) 4558–4576.
[5] F. Scheller, F. Schubert, Biosensor, Elsevier, New York, 1992.
[6] D.E. Reed, F.M. Hawkridge, Anal. Chem. 59 (1987) 2334–2339.
[7] X. Chen, J. Hu, Z. Chen, X. Feng, A. Li, Biosens. Bioelectron. 24 (2009) 3448–3454.
[8] F. Gao, Z. Yao, Q. Huang, X. Chen, X. Guo, Q. Ye, L. Wang, Colloids Surf. B 82 (2011) 359–364.
[9] W. Zheng, Y.F. Zheng, K.W. Jin, N. Wang, Talanta 74 (2008) 1414–1419.
[10] W. Zheng, J. Li, Y.F. Zheng, Biosens. Bioelectron. 23 (2008) 1562–1566.
[11] P. Lo, S.A. Kumar, S. Chen, Colloids Surf. B 66 (2008) 266–273.
[12] X. Luo, A.J. Killard, M.R. Smyth, Electroanalysis 18 (2006) 1131–1134.
[13] X.D. Zeng, X.F. Li, L. Xing, X.Y. Liu, S.L. Luo, W.Z. Wei, B. Kong, Y.H. Li, Biosens. Bioelectron. 24 (2009) 2898–2903.
[14] A. Ressine, C. Vaz-Dominguez, V.M. Fernandez, A.L. De Lacey, T. Laurell, T. Ruzgas, S. Shleev, Biosens. Bioelectron. 25 (2010) 1001–1007.
[15] Y. Wang, X.L. Ma, Y. Wen, Y.Y. Xing, Z.R. Zhang, H.F. Yang, Biosens. Bioelectron. 25 (2010) 2442–2446.
[16] H. Guo, D. Liu, X. Yu, X. Xia, Sens. Actuators B: Chem. 139 (2009) 598–603.
[17] M. Shamsipur, S.H. Kazemi, M.F. Mousavi, Biosens. Bioelectron. 24 (2008) 104–110.
[18] B.Z. Jang, A. Zhamu, J. Mater. Sci. 43 (2008) 5092–5101.
[19] S. Alwarappan, C. Liu, A. Kumar, C.Z. Li, J. Phys. Chem. C 114 (2010) 12920–12924.
[20] W. Zheng, H.Y. Zhao, J.X. Zhang, H.M. Zhou, X.X. Xu, Y.F. Zheng, Y.B. Wang, Y. Cheng, B.Z. Jang, Electrochem. Commun. 12 (2010) 869–871.
[21] C.X. Guo, Z.S. Lu, Y. Lei, C.M. Li, Electrochem. Commun. 12 (2010) 1237–1240.
[22] Y.X. Fang, S.J. Guo, C.Z. Zhu, Y.M. Zhai, E.K. Wang, Langmuir 26 (2010) 11277–11282.
[23] J.F. Wang, S.L. Yang, D.Y. Guo, P. Yu, D. Li, J.S. Ye, L.Q. Mao, Electrochem. Commun. 11 (2010) 1892–1895.
[24] L.A. Palomares, M. Gonzalez, O.T. Ramirez, Enzyme Microb. Technol. 26 (2000) 324–331.
[25] Z. Wei, J. Hao, S. Yuan, Y. Li, W. Juan, X. Sha, X. Fang, Int. J. Pharm. 376 (2009) 176–185.
[26] D.Y. Alaknova, N.Y. Rapoport, E.V. Batrakova, A.A. Timoshin, S. Li, D. Nicholls, V.Y. Alakhov, A.V. Kabanov, J. Control. Release 142 (2010) 89–100.
[27] N. Jia, Q. Lian, Z. Wang, H. Shen, Sens. Actuators B: Chem. 137 (2009) 230–234.
[28] S.S. Razola, B.L. Ruiz, N.M. Diez, H.B. Mark, J.-M. Kauffmann, Biosens. Bioelectron. 17 (2002) 921–928.
[29] Q. Deng, S.J. Dong, J. Electroanal. Chem. 377 (1994) 191–195.
[30] J.B. Matthew, G.I. Hanania, F.R. Gurd, Biochemistry 18 (1979) 1919–1928.
[31] J.C. Meyer, A.K. Geim, M.I. Katsnelson, K.S. Novoselov, T.J. Booth, S. Roth, Nature 446 (2007) 60–63.
[32] G. Wang, J. Yang, J. Park, X. Gou, B. Wang, H. Liu, J. Yao, J. Phys. Chem. C 112 (2008) 8192–8195.
[33] A.F. Nassar, Z. Zhang, N. Hu, J.F. Rusling, T.F. Kumosinski, J. Phys. Chem. B 101 (1997) 2224–2231.
[34] Z. Zhang, S. Chouchane, R.S. Magliozzo, J.F. Rusling, Anal. Chem. 74 (2002) 163–170.
[35] E. Laviron, J. Electroanal. Chem. 61 (1979) 19–28.
[36] H.Y. Zhao, W. Zheng, Z.X. Meng, H.M. Zhou, X.X. Xu, Z. Li, Y.F. Zheng, Biosens. Bioelectron. 24 (2009) 2352–2357.
[37] H.Y. Zhao, X.X. Xu, J.X. Zhang, W. Zheng, Y.F. Zheng, Bioelectrochemistry 78 (2010) 124–129.
[38] G. Zhao, J.J. Feng, J.J. Xu, H.Y. Chen, Electrochem. Commun. 7 (2005) 724–729.
[39] F. Yin, H.K. Shin, Y.S. Kwon, Talanta 67 (2005) 221–226.
[40] I. Yamazaki, T. Araiso, Y. Hayashi, H. Yamada, R. Makino, Adv. Biophys. 11 (1978) 249–281.
[41] W. Zheng, J. Li, Y.F. Zheng, J. Electroanal. Chem. 621 (2008) 69–74.
[42] M. Fedurco, J. Augustynski, C. Indiani, G. Smulevich, M. Antalik, M. Bano, E. Sedlak, M.C. Glascock, J.H. Dawson, J. Am. Chem. Soc. 127 (2005) 7638–7646.
[43] Z. Mai, X. Zhao, Z. Dai, X. Zou, Talanta 81 (2010) 167–175.
[44] C. Lie, U. Wollenberger, M. Gheorghe, A. Guiseppi-Elie, F. Scheller, Anal. Bioanal. Chem. 372 (2002) 235–239.
[45] J. You, W. Ding, S. Ding, H. Ju, Electroanalysis 21 (2009) 190–195.
[46] H.Y. Xiao, H.X. Lu, H.Y. Chen, Anal. Biochem. 278 (2000) 22–28.
[47] Y. Wang, X. Chen, J. Zhu, Electrochem. Commun. 11 (2009) 323–326.
[48] W. Ma, D. Tian, Bioelectrochemistry 78 (2010) 106–112.
[49] Y. Li, Q. Zhang, J. Li, Talanta 83 (2010) 162–166.
[50] N. Zheng, X. Zhou, W. Yang, X. Li, Z. Yuan, Talanta 79 (2009) 780–786.
[51] R.A. Kamin, G.S. Wilson, Anal. Chem. 52 (1980) 1198–1205.
[52] M.C. Liu, G.H. Zhao, K.J. Zhao, X.L. Tong, Y.T. Tang, Electrochem. Commun. 11 (2009) 1379–1400.
[53] Y. Li, X. Zeng, X. Liu, X. Liu, W. Wei, S. Luo, Colloids Surf. B 79 (2010) 241–245.
[54] L. Liu, B. Shen, J. Shi, F. Liu, G. Lu, J. Zhu, Biosens. Bioelectron. 25 (2010) 2627–2632.
[55] X. Lu, Y. Xiao, Z. Lei, J. Chen, Biosens. Bioelectron. 25 (2009) 244–247.
[56] K. Huang, J. Sun, D. Niu, W. Xie, W. Wang, Colloids Surf. B 78 (2010) 69–74.